Migration of Retinal Cells through a Perforated Membrane: Implications for a High-Resolution Prosthesis

Daniel Palanker[1,2], Philip Huie[1,2], Alexander Vankov[2], Robert Aramant[3], Magdalene Seiler[3,4], Harvey Fishman[1], Michael Marmor[1], Mark Blumenkranz[1]

[1] Department of Ophthalmology, School of Medicine, Stanford University, Stanford, CA;

[2] W.W. Hansen Experimental Physics Laboratory, Stanford University, Stanford, CA;

[3] Doheny Retina Institute, Depts. of Ophthalmology and [4] Cell & Neurobiology, School of Medicine, University of Southern California.

Word count: 2,620

Figures: 7

Section code: RE

Keywords: retinal prosthesis, neuronal remodeling, age-related macular degeneration, retinitis pigmentosa

Corresponding author: Daniel Palanker

Address: W.W. Hansen Experimental Physics Laboratory, Stanford University, Stanford, CA, 94305-4085.

Tel: (650) 725-0059, Fax: (650) 725-8311

E-mail: palanker@stanford.edu

This work was funded in part by the Stanford University Bio-X grant and by VISX Inc.

CR: F, P

Abstract

Purpose: One of the critical issues in design of a high-resolution retinal implant is the proximity of stimulating electrodes to the target cells. We report on a phenomenon of retinal cellular migration into a perforated membrane that may help to address this issue.

Methods: Mylar membranes with an array of perforations (3-40 microns in diameter), were used as a substrate for *in-vitro* retinal culture (chicken, rats), and were also transplanted into the subretinal space of adult RCS rats. A membrane was also constructed with a seal on one side to restrict the migration.

Results: Retinal tissue *in-vitro* grew within 3 days through perforations of greater than 5μm in diameter when the membranes were positioned on the photoreceptor side, but no migration occurred if the implant was placed on the inner retinal surface. Histology with light microscopy and TEM demonstrated that migrating cells retain neuronal structures for signal transduction. Similar growth of RCS rat retinal cells occurred *in-vivo* within 5 days of implantation. A basal seal kept the migrating tissue within a small membrane compartment.

Conclusions: Retinal neurons migrate within a few days into perforations (>5 μm in diameter) of a membrane placed into the subretinal space. This may provide a means of gaining close proximity between electrodes in a retinal prosthetic chip and target cells, and thus allow a greater density of stimulating elements to subserve higher resolution. Further studies are needed to explore the long-term stability of the retinal migration.

Introduction

As the population ages, vision loss from retinal diseases is becoming a major public health issue. Two degenerative retinal disorders are the current focus of retinal prosthetic work: retinitis pigmentosa (RP) and age-related macular degeneration (AMD). In these diseases, the photoreceptor layer of the retina degenerates, yet the "processing circuitry" and "wiring" are at least to some degree preserved. If one could bypass the photoreceptors and directly stimulate the inner retina with visual signals, one might be able to restore sight[1-4]. Some first steps have been taken towards the development of an electronic retinal prosthesis. Human patients stimulated with an array of 16 - 20 electrodes of 0.4mm in size can recognize reproducible visual percepts [3, 5], which gives hope that with some learning and image processing the patients might be able to get used to this type of stimulation[6]. Electrical stimulation of neural cells in the retina has been achieved with an array of electrodes positioned on either the inner[4, 5, 7, 8] or outer side of retina[9-11]. Setting the electrodes into the subretinal space with electrical stimulation of the inner retinal cells, although surgically challenging, has the potential advantage that earlier signal processing in the retina may be partially preserved, relative to the excitation of ganglion cells with electrodes positioned on the epiretinal side. These pioneering implants are a long way from the numbers and densities of stimulating pixels needed to achieve functional levels of vision. (We must emphasize though that high density of retinal stimulation is only one of the requirements for restoring useful visual perception.)

Implantation will be worth its risk for patients with low visual acuity (e.g. 20/400) only if it provides substantial improvement. A visual acuity of 20/80 corresponds geometrically to a pixel size of 20 μm and pixel density of 2500 pixels/mm^2 [12]. To achieve such high resolution stimulation it will be necessary to bring the prosthetic electrodes close to the target cells. This

problem has hardly been addressed. Simple placement of a flat electrode array on, or under, the retina always leaves a large distance between electrodes and cells because the inner limiting membrane and nerve fiber layer intervene in the case of epiretinal approach, and photoreceptor remnants interfere in the case of sub-retinal implantation. In addition, diseased retina may have uneven thickness or a wavy structure. Large distances between the cells and electrodes require a high charge density and power for cell stimulation [12] and result in cross-talk between closely-spaced electrodes. High charge density and power can lead to erosion of electrodes and excessive heating of the tissue, all of which limit spatial resolution. Furthermore, any variability in the distance between electrodes and cells in different parts of the implant will result in variations of the stimulation threshold, making it necessary to adjust the signal intensity in each pixel. We have recently calculated [12] that for chronic stimulation with a pixel density of 400 pixels/mm^2, which geometrically corresponds to visual acuity of 20/200, the electrodes need to be within 15-20 μm of the target neurons. For visual acuity of 20/80, the separation between electrodes and target cells should not exceed 7μm. Thus, ensuring a very close proximity of retinal cells to the stimulating electrodes is one of the important issues, and challenges, in the design of a high resolution retinal prosthesis.

Our laboratory is exploring several approaches to ensure proximity of neural cells to stimulating electrodes [13-15]. In this paper we report that a subretinal placement of a perforated membrane will prompt a migration of retinal cells through the perforations.

Material and Methods

(A) In-vitro experiments

Mylar membrane, 13 μm in thickness, was perforated on an inverted microscope using tightly focused beam of a picosecond Ti-Sapphire laser (Spitfire, Spectra Physics, Inc., Santa Clara, CA). Aperture sizes were varying in the range of 3 to 40 μm. The surface of the membrane was treated with 0.1 mg/ml poly-l-lysine (P2636, Sigma, St. Louis, MO) and 0.4 mg/ml laminin diluted in Neurobasal Medium (L2020, Sigma, St. Louis, MO, and Gibco BRL, Carlsbad, CA, respectively). The perforated membranes were affixed atop polystyrene rings mounted at the center of Petri dishes to form an inner chamber and a surrounding outer chamber. The inner and outer chambers were filled with the same culture media. Some membranes were constructed with an additional Mylar basal membrane with and without 3μm perforations to limit retinal cellular migration.

Animals were used in accordance with the ARVO Statement Regarding the Use of Animals in Ophthalmic and Vision Research. Retinas were harvested from P7 Sprague-Dawley rat pups (20 samples) and from 16-18 day chicken embryos (6 samples). After removal of ILM by peeling the retinas were positioned onto perforated Mylar membranes and incubated for 72 hours in growth media that consisted of Neurobasal Media, pen/strep, insulin, L-glutamine, Sato, and B27. Each membrane had an array of 20 to 50 apertures (4x5 to 5x10). Tuft growth through the perforations was visually monitored with a Nikon TS100 inverted microscope and then processed for histological examination.

(B) In-vivo experiments

Five albino Royal College of Surgeons (RCS) rats, derived from the breeding colony at Doheny Eye Institute, CA, received implants into one eye at the age of 63 days. The implantation procedure have been described in detail elsewhere [16]. In anesthetized rats (Ketamine 37.5

mg/kg; Xylazine 5 mg/kg), a small incision (~1 mm) was cut trans-sclerally behind the pars plana of the host eye, and the perforated Mylar film (0.8x1.5 mm in size) was placed into the subretinal space, in the back of the eye near the optic disc in the nasal or superior nasal quadrant of the host, using a custom-made implantation tool. Each implant had an array of 28 apertures (4x7). Placement of the transplants was evaluated after each surgery by fundus examination. One surgery failed, and the other four rats were sacrificed for histological analysis in the following order: two rats were sacrificed on the 5th day, one on 7th and one on 9th day after surgery.

(C) Histology

Retina/perforated membranes in the in-vitro experiments and the enucleated eyes in the in-vivo experiments were immersion-fixed in 2.5 % glutaraldehyde/2.0 % paraformaldehyde in 0.1 M sodium cacodylate buffer, pH 7.4 or in 0.1 M sodium phosphate buffer, pH 7.2. The cornea in the RCS rat eyes was removed 20 – 50 min. later, and the eyes were postfixed overnight at 4°C. The tissue was washed in 0.1 M sodium cacodylate or 0.1 M sodium phosphate, osmicated in 2% osmium tetroxide, dehydrated in a series of ethanols and washed in anhydrous propylene oxide.

The tissues were embedded in either EMbed 812 (Electron Microscopy Sciences, Port Washington, PA) or LX-112 (Ladd Research Industries, Inc., Burlington, VT). One micron sections for light microscopy or 100 nm sections for transmission electron microscopy were cut on a Reichert-Jung Ultracut E ultramicrotome (Leica, Deerfield, IL). Sections for light microscopy were stained with toluidine blue and photographed on Nikon Eclipse E1000 microscope (Nikon Instruments, Inc., New York, NY). Thin sections for electron microscopy

were stained with uranyl acetate and lead citrate. Transmission electron micrographs were collected with a JEOL 1230 (JEOL USA, Inc., Peabody, MA).

Results

In-vitro experiments with 14 P7 rats were performed with 12 membranes (having each an array of 28-40 apertures of 3 - 30 μm in size, total 383 apertures) placed subretinally – i.e. photoreceptor-side down, and 2 membranes (having arrays of 28 and 30 apertures of 5 - 30 μm in size) epiretinally. 72 hours after the explantation migration was observed in 88% of the subretinal apertures larger than 5μm in size. Migration did not occur through the apertures of 5 μm or smaller, nor did it occur with any aperture sizes after epiretinal placement. In-vitro experiments with chicken retina have been performed with 6 membranes each having 40 apertures of 10 - 20 μm in size, all of which where placed subretinally. At 72 hours after the explantation migration was observed in 81% of the apertures.

Histologic results obtained in-vitro with the P7 rat retinas are shown in Figures 1-3. Migration of cells from the outer nuclear layer, outer plexiform layer and inner nuclear layer progressively increased with the aperture sizes above 5 μm. The cellular invasion of the aperture appeared to include both glial and neural cellular elements. As shown in Figure 1B, the extent of tissue migration increased with the size of the aperture. A transmission electron micrograph of a section through an aperture (similar to the line A-B, in Figure 1A) is shown in Figure 2, and demonstrates the presence of neuronal processes (axons or dendrites) connecting the migrating cells. These finding indicate the possibility of signal transmission between stimulated cells in the aperture and cells in the rest of the retina.

Figure 3 demonstrates a typical example of culturing the rat retina upside down, i.e. nerve fiber layer towards the membrane, that did not result in cellular migration even though the ILM was peeled off.

The RCS rat was chosen as a model for *in-vivo* experiments, since they retina is vascularized and the photoreceptors degenerate as in RP. Results of the experiments with subretinal Mylar films perforated with 4x7 arrays of apertures of 15 - 40 μm in size have been analyzed histologically in 4 eyes from the animals sacrificed 5, 7 and 9 days after the implantation. A robust migration of the inner nuclear layer was observed in all 36 apertures analyzed histologically (Figures 4 and 5). In several apertures we also observed a migration of retinal capillaries into the pore (Figure 5).

Since unlimited tissue migration through a membrane could be problematic (draining retinal cells and proliferating under the prosthesis) we explored the placement of perforated membranes with a basal seal to prevent growth out the bottom (Figure 6). To test whether diffusion of nutrients is essential for migration some of the basal Mylar membranes where perforated, and some were not. The experiments were performed in-vitro with 6 cultured P7 rat retinas using 6 devices having each an array of 15 (5x3) chambers. 9 out of 15 chambers in each device had small perforations (3 μm) at the basal membrane, and 6 did not. When retinas were cultured over these 3-layer structures for 7-14 days, tissue was observed to migrate into 94% of chambers with basal perforations (Figure 6B), and 87% of those with no basal perforations (Figure 7). One can see in both of these Figures that the nuclei of the outer nuclear layer are migrating into the chamber.

Discussion

The remodeling and potential plasticity of adult retina after injury or degeneration of the photoreceptors has been documented now by many investigators [17-22]. There is not only neuronal proliferation but also a growth of non-neural cells including Muller cells and blood vessels[17-22]. After retinal reattachment, Muller cell processes and displaced photoreceptor nuclei can move into the sub-retinal space and spread laterally[18, 19]. The cell processes of displaced Muller cells can form scaffolds that aid in the migration of other retinal neural cells[20], and these may be facilitating the neural retinal migration in our case. Another mechanism of retinal migration involves permeation of the RPE cell extensions deep into the neural retina, and the attraction of small blood vessels from the ganglion cell layer [21]. However, RPE cannot be responsible for the retinal migration we observed in-vitro since no RPE was present in that case. The participation of the RPE cells in-vivo will also be prevented if a membrane seals the bottom of an implant, as shown in Figures 6 and 7.

The relevance of these observations to prosthetic chip technology is that while close spacing of electrodes on a chip is needed for high resolution, there will be electrode cross-talk or excessive power requirements unless the target neurons come within a few microns of the stimulus area. Since retinal neurons enter a perforated membrane, as we have shown, they would enter a chip that has stimulating electrodes in perforations (as suggested in Figure 6A). This would bring the electrodes and neurons into close proximity, which is necessary for high-resolution performance. Penetration of cells into the pores of an implant may also help to achieve a firm mechanical anchoring of the device to tissue.

Effect of cellular migration can also be utilized with an implant having an array of thin protruding electrodes insulated at their sides and exposed at the tops. When positioned under the retina, the cells will migrate into the empty spaces between the electrodes thus assuring

penetration of the electrodes into the retina without high pressure and associated risk of mechanical injury. The depth of penetration will be determined by the length of the electrodes. The approaches based on pores and on protruding electrodes are complimentary: in the first case the actively migrating cells penetrate into the pores and will be stimulated. In the second case the actively migrating cells move towards the bottom of an implant, while the electrodes penetrate deep into the retina approaching the target cells which did not migrate and remained in place.

Major concerns with retinal migration are whether the neural cells that move into the pores will survive for an extended period of time, and whether the organization of the migrated tissue will change through glial overgrowth or cell death. Studies with non-porous sub-retinal implants suggest that the Muller cells can migrate and proliferate, making fibrous tissue and changing neuronal configurations [22, 23]. Proliferation of the glial cells has also been observed with porous membranes implanted on the epiretinal side[24]. We plan to study the long-term behavior of retinal cells migrating into perforated implants, and to optimize their structure for preserving neural connections and assuring efficacy of an electric interface. Our purpose in this initial report is simply to alert readers to this intriguing phenomenon of neural ingrowth, and to emphasize its potential relevance to prosthetic chip development.

Acknowledgements

Authors would like to thank Kalayaan V. Bilbao and Dimitri Yellachich for help with the rabbit surgery, and Zhenhai Chen for help with the rat surgeries. Thomas Guillaume, Yevgeny Freyvert and Gary Chern for help with membrane fabrication and Roopa Dalal for histological preparations.

Funding is provided in part by the Stanford University Bio-X grant and by the VISX Inc. The work at Doheny was supported by an Anonymous sponsor, the Foundation for Fighting Blindness and NIH EY03040 (core grant).

References

1. Zrenner, E., *Will retinal implants restore vision?* Science, 2002. **295**(5557): p. 1022-1025.
2. Humayun, M.S. and E. de Juan, *Artificial vision.* Eye, 1998. **12**: p. 605-607.
3. Humayun, M.S. *Clinical Trial Results with a 16-Electrode Epiretinal Implant in End-Stage RP Patients*. in *The First DOE International Symposium on Artificial Sight*. 2003. Fort Lauderdale, FL: Department of Energy.
4. Margalit, E., et al., *Retinal prosthesis for the blind.* Survey of Ophthalmology, 2002. **47**(4): p. 335-356.
5. Rizzo, J.F., 3rd, et al., *Perceptual efficacy of electrical stimulation of human retina with a microelectrode array during short-term surgical trials.* Invest Ophthalmol Vis Sci, 2003. **44**(12): p. 5362-9.
6. Humayun, M.S., et al., *Visual perception in a blind subject with a chronic microelectronic retinal prosthesis.* Vision Research, 2003. **43**(24): p. 2573-81.
7. Margalit, E., et al., *Visual and electrical evoked response recorded from subdural electrodes implanted above the visual cortex in normal dogs under two methods of anesthesia.* Journal of Neuroscience Methods, 2003. **123**(2): p. 129-137.
8. Humayun, M.S., et al., *Pattern electrical stimulation of the human retina.* Vision Research, 1999. **39**(15): p. 2569-2576.
9. Zrenner, E., et al., *Subretinal microphotodiode arrays to replace degenerated photoreceptors?* Ophthalmologe, 2001. **98**(4): p. 357-363.
10. Stett, A., et al., *Electrical multisite stimulation of the isolated chicken retina.* Vision Research, 2000. **40**(13): p. 1785-1795.
11. Sachs, H.G., et al., *Subretinal implantation of electrodes for acute in vivo stimulation of the retina to evoke cortical responses in minipig.* Investigative Ophthalmology & Visual Science, 2000. **41**(4): p. S102-S102.
12. Palanker, D., et al., *Physical Constraints on the Design of a High-Resolution Electronic Retinal Prosthesis.* Invest Ophthalmol Vis Sci, 2003. **submitted**.
13. Huie, P., et al., *Tissue-engineered Neurite Conduits to Connect Retinal Ganglion Cells to an Electronic Retinal Prosthesis.* Investigative Ophthalmology and Visual Science, 2002. **43**: p. E-Abstract 4475.
14. Huie, P., et al., *Perforated Membrane as an Interface for Focal Electrical Stimulation of Retina.* Investigative Ophthalmology and Visual Science, 2003. **44**: p. E-Abstract 5055.
15. Peterman, M.C., et al., *The Artificial Synapse Chip: A Flexible Retinal Interface Based on Directed Retinal Cell Growth and Neurotransmitter Stimulation.* Artificial Organs, 2003. **27**(11): p. 975-985.
16. Aramant, R.B. and M.J. Seiler, *Retinal transplantation--advantages of intact fetal sheets.* Prog Retin Eye Res, 2002. **21**(1): p. 57-73.
17. Fisher, S.K., et al., *Intraretinal proliferation induced by retinal detachment.* Invest Ophthalmol Vis Sci, 1991. **32**(6): p. 1739-48.
18. Erickson, P.A., et al., *Retinal detachment in the cat: the outer nuclear and outer plexiform layers.* Invest Ophthalmol Vis Sci, 1983. **24**(7): p. 927-42.
19. Anderson, D.H., et al., *Morphological recovery in the reattached retina.* Invest Ophthalmol Vis Sci, 1986. **27**(2): p. 168-83.

20. Sullivan, R., P. Penfold, and D.V. Pow, *Neuronal migration and glial remodeling in degenerating retinas of aged rats and in nonneovascular AMD.* Investigative Ophthalmology & Visual Science, 2003. **44**(2): p. 856-65.
21. Villegas-Perez, M.P., et al., *Ganglion cell loss in RCS rat retina: a result of compression of axons by contracting intraretinal vessels linked to the pigment epithelium.* J Comp Neurol, 1998. **392**(1): p. 58-77.
22. Marc, R.E., et al., *Neural remodeling in retinal degeneration.* Prog Retin Eye Res, 2003. **22**(5): p. 607-55.
23. Pardue, M.T., et al., *Immunohistochemical studies of the retina following long-term implantation with subretinal microphotodiode arrays.* Exp Eye Res, 2001. **73**(3): p. 333-43.
24. Laube, T., et al., *Biochemical fixation: A new type of epi-retinal implant fixation.* Investigative Ophthalmology and Visual Science, 2000. **41**(4, suppl.S): p. S102-S102.

Figures

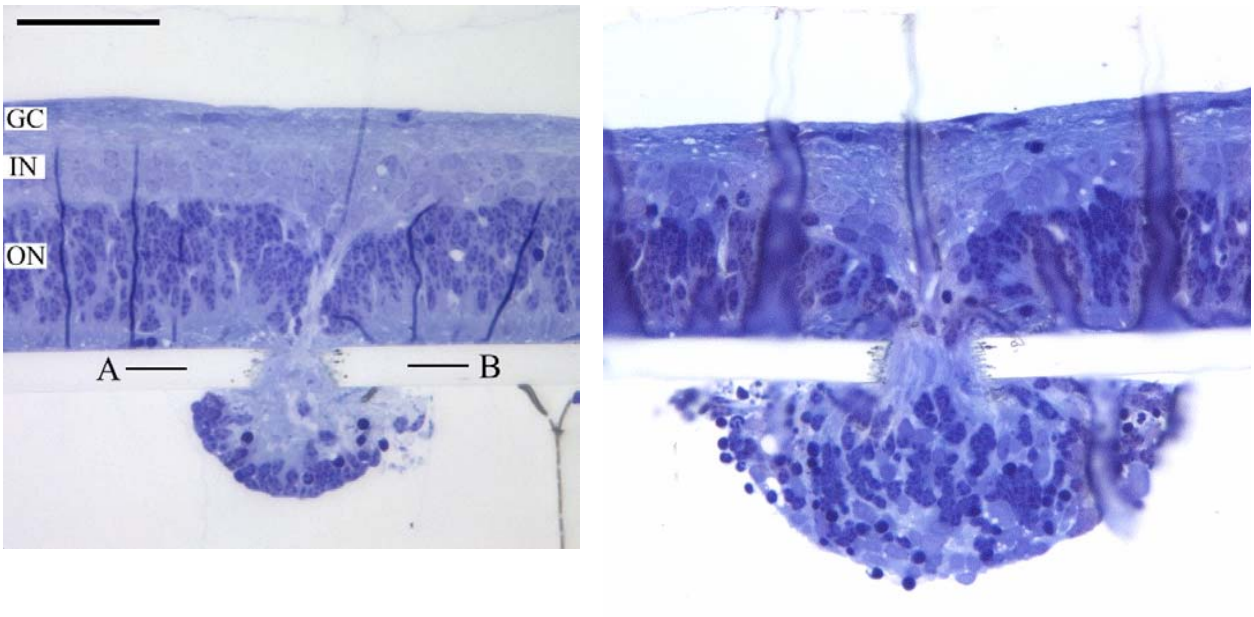

Figure 1. Light micrographs of the histological sections of the P7 rat retina 72 hours after explantation onto 13 μm-thick perforated Mylar membrane. Left aperture is 16 μm in diameter, the right one is 26 μm. The cellular migration is greater through the larger aperture. Scale bar is 50 μm. Letters A and B in the left frame indicate the line of sectioning for TEM imaging of the tuft shown in Figure 2. Retinal layers are labeled with the two-letter code as following: CG – ganglion cell layer, IP – inner plexifom layer, IN - inner nuclear layer, OP – outer plexiform layer, ON – outer nuclear layer, PE – retinal pigmented epithelium, CH – choroid. M – migrated tissue.

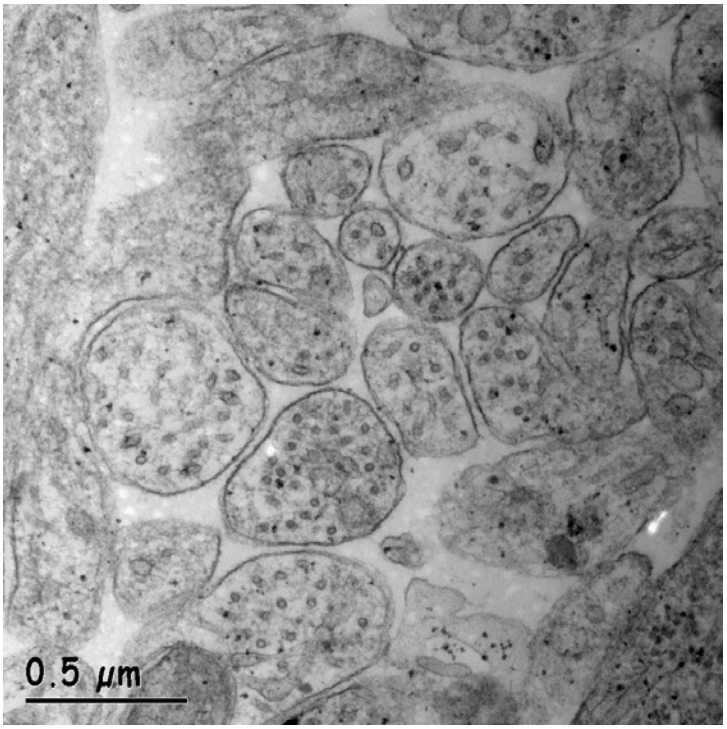

Figure 2. TEM: Cross-section of nerve axons or dendrite within a channel connecting cells within the retina to a migrating tuft. Scale bar is 0.5 μm.

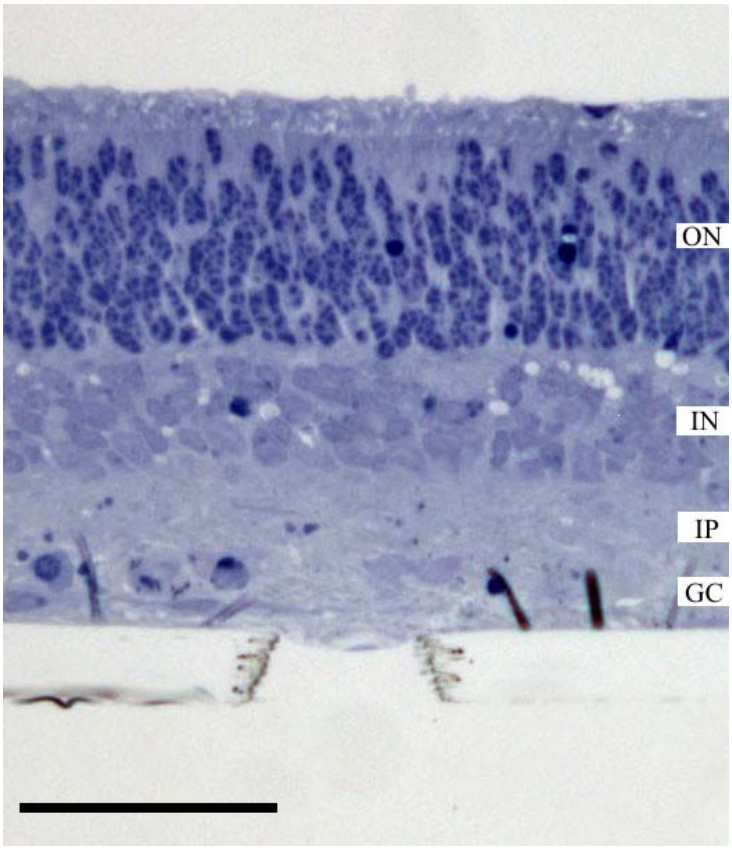

Figure 3.

P7 rat retina cultured for 72 hours in-vitro "upside down", i.e. with the NFL adjacent to the perforated membrane. No cellular migration was observed with the pore sizes up to 23 μm. Scale bar is 50 μm. Labeling of the retinal layers is described in the caption of Figure 1.

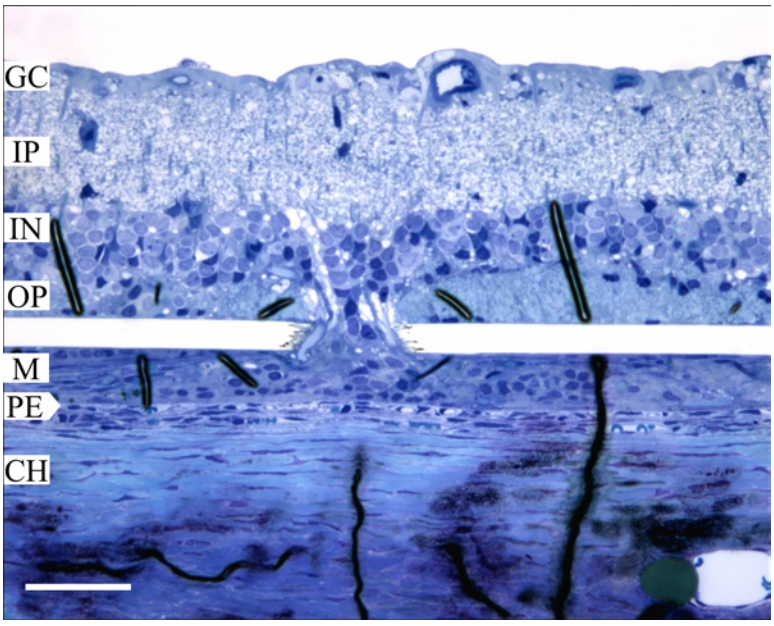

Figure 4. Histological section of the RCS rat retina 9 days after implantation of the perforated Mylar membrane into the sub-retinal space. Retinal tissue migrates through the hole and spreads between the RPE and the membrane. Scale bar is 50 μm. Labeling of the retinal layers is described in the caption of Figure 1.

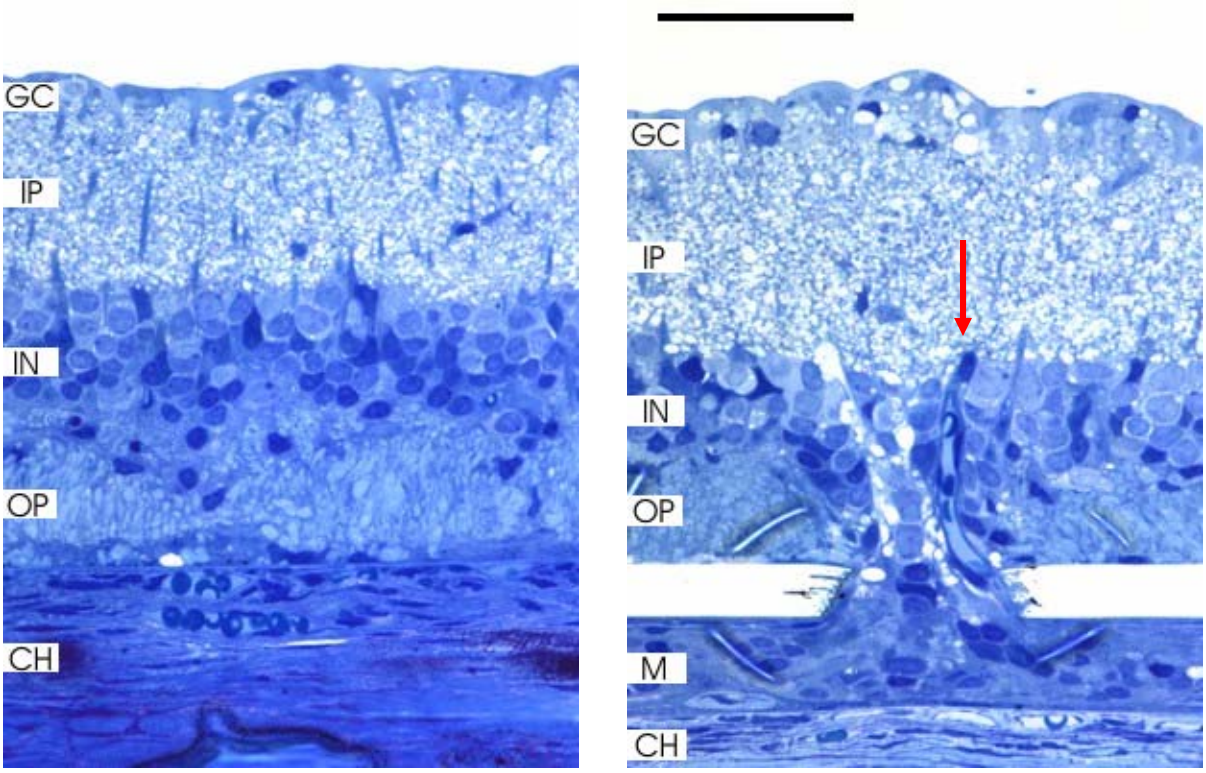

Figure 5. Histological sections of the RCS rat retina 9 days after implantation. **Left:** Normal appearance of the RCS rat retina far from the implant. **Right:** Retinal tissue migrates through the aperture of 40 µm and spreads between the RPE and the membrane. An arrow points to a blood capillary migrating into the pore. Scale bar 50 µm. Labeling of the retinal layers is described in the caption of Figure 1.

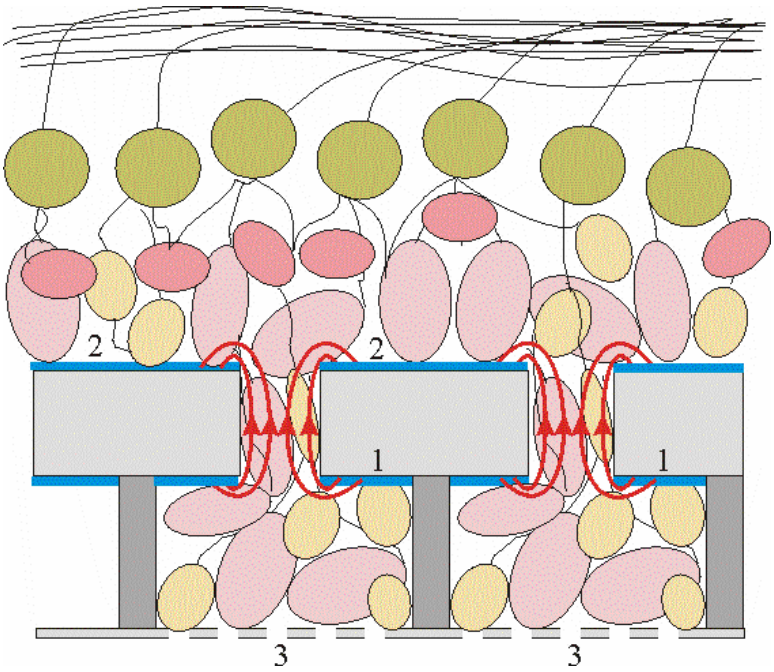

Figure 6A.

Schematic representation of a 3-layered membrane having an entry channel on top, a wider inside chamber, and a fenestrated membrane (3) at the bottom to limit cellular migration. Stimulating voltage could be applied between an inner electrode (1) and a common return electrode (2).

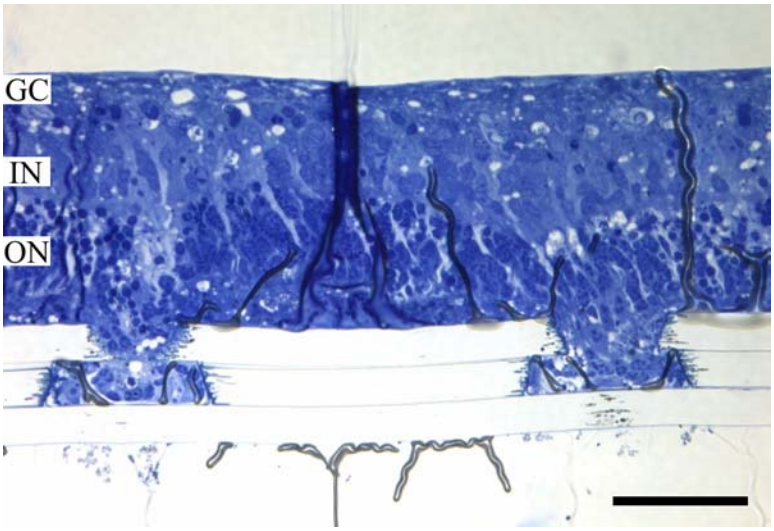

Figure 6B.

Rat retina grown on the 3-layered structure for 7 days in-vitro. Retinal cells migrated through the 20 and 35 μm holes into the middle chambers of 60 μm in width, but cannot penetrate through the 3 μm holes in the lower membrane. Scale bar is 50 μm. Labeling of retinal layers is as in caption of Figure 1.

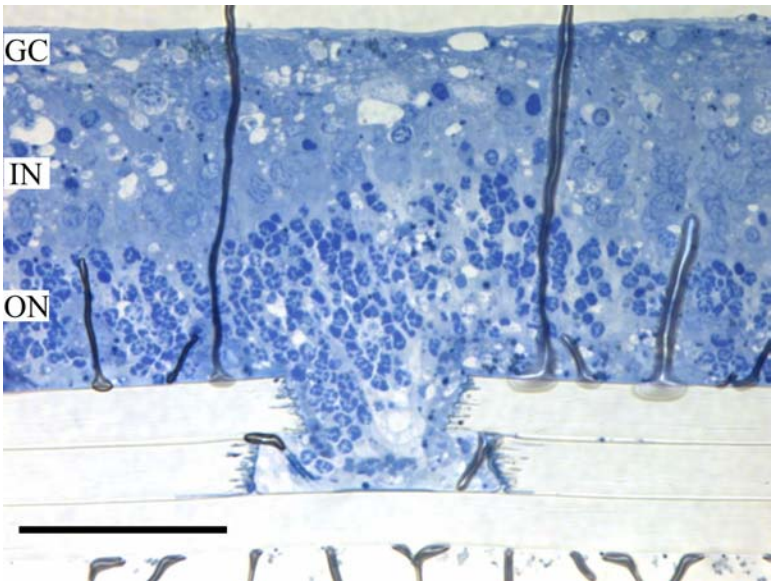

Figure 7.

Rat retina grown on the 3-layered structure for 7 days in-vitro. Retinal cells migrated through the 35 μm holes into the middle chambers of 60 μm in width, which did not have holes in the lower membrane. Scale bar is 50 μm. Labeling of the retinal layers is described in the caption of Figure 1.